Dicle University
Journal of Engineering
https://dergipark.org.tr/tr/pub/dumf
duje.dicle.edu.tr

Research Article

Energy and Exergy Analysis of a Metal Hydride-Based Hydrogen Storage System: A Parametric Approach

Nesrin İLGİN BEYAZİT[1*]

[1]Dicle University, Electrical-Electronics Engineering Department, nesrinilgin@gmail.com, Orcid No: 0000-0003-4708-9615

ARTICLE INFO

Article history:

Received 1 August 2025
Received in revised form 3 November 2025
Accepted 19 November 2025
Available online 30 December 2025

Keywords:

Hydrogen storage, Metal hydride reactor, Energy analysis, Exergy efficiency, Parametric study, Thermal management

Doi: 10.24012/dumf.1756471

* Corresponding author

ABSTRACT

Hydrogen is considered a promising energy carrier for the global energy transition due to its high energy density and environmental sustainability. However, the efficient storage of hydrogen remains a major technical challenge that limits its large-scale deployment. Metal hydrides (MHs) offer a safe and compact solution, but their thermal management strongly influences storage efficiency.This study conducts a comprehensive energy and exergy analysis of a magnesium hydride (MgH_2)-based storage system to evaluate the combined influence of key parameters: reactor number, outlet temperature, coolant mass flow rate, pump efficiency, ambient temperature, heat transfer coefficient, hydrogen capacity, and the volume-to-surface (V/A) ratio. The numerical model integrates energy–exergy formulations to quantify performance under different operating conditions.The results reveal that increasing the number of reactors enhances exergy efficiency from 21.5% to 64.9%, while higher outlet temperatures and mass flow rates reduce efficiency due to thermal imbalance and pumping losses. In contrast, improving the heat transfer coefficient up to 3000 $W/m^2 \cdot K$ increases efficiency to 73.9%, demonstrating the critical role of thermal design.These findings provide design guidelines for optimizing reactor configuration, flow management, and material selection. The study offers practical insights for engineering applications and supports the development of scalable, high-efficiency MH-based hydrogen storage systems.

Introduction

The global transition toward sustainable energy systems has intensified efforts to reduce dependence on fossil fuels and mitigate environmental degradation. In this context, hydrogen has emerged as a promising energy carrier due to its high gravimetric energy density, environmental friendliness, and flexibility in various applications such as transportation, power generation, and industrial processes [1], [2]. However, one of the major challenges hindering its large-scale adoption is the safe, efficient, and compact storage of hydrogen [3], [4].

Hydrogen can be stored through different methods, including compressed gas, cryogenic liquid storage, chemical carriers, and solid-state materials such as metal hydrides (MHs) [5], [6]. Among these, MH-based systems are particularly attractive because they can store hydrogen at moderate pressures with high volumetric density and enhanced operational safety [7]. Recent developments in MgH_2- and TiFe-based materials, driven by nanostructural engineering and alloy modification, have enhanced reaction kinetics and cycling stability [8]–[10]. In parallel, high-entropy alloys (HEAs) have emerged as new candidates for reversible hydrogen storage due to their tunable thermodynamic and mechanical properties [11]–[13].

Thermal management is a key factor that determines the performance of MH reactors. Efficient removal or supply of heat during absorption and desorption directly influences hydrogen kinetics and overall system efficiency [14], [15]. Hence, parameters such as reactor configuration, heat exchanger geometry, coolant mass flow rate, ambient temperature, and the volume-to-surface area (V/A) ratio are crucial for optimizing energy and exergy performance [16]–[18].

Numerous experimental and numerical studies have explored these aspects. For example, Jana and Muthukumar developed a 19-tube bundle reactor (TBR) capable of storing 369 g of hydrogen with 64% energy efficiency under moderate pressures [19], [20]. Parashar and Muthukumar (2024) achieved 82.3% efficiency in a compact multi-tube reactor using Ti–Zr–Mn–V–Fe alloys [21]. Raju and Kumar (2011) demonstrated that helical tube designs, simulated through COMSOL–MATLAB coupling, provide superior heat transfer performance compared to straight tubes [22]. Bai et al. (2021) optimized fin geometries and reduced absorption time by 20.7%, while Liu et al. (2022) showed that multi-heat-transfer-tube (MHTT) designs further improve heat distribution and overall efficiency [23], [24].

Despite these advancements, most existing research has primarily focused on geometric optimization or material enhancement [18], [25]. Comprehensive exergy-based evaluations that simultaneously consider multiple design and operating parameters remain limited [26]. Only a few studies—such as Nyallang and Tolj (2021)—have examined trade-offs between pump power and efficiency, emphasizing the necessity of a comprehensive performance assessment [27].

Therefore, this study comprehensively analyzes the effects of key parameters — such as the number of reactors, inlet temperature of the cooling fluid, mass flow rate, pump efficiency, ambient temperature, heat transfer coefficient, hydrogen loading capacity, and reactor volume-to-surface (V/A) ratio — on the energy and exergy performance of the system. In this context, not only the first-law efficiency but also the second-law (exergy) efficiency is evaluated from a multi-dimensional perspective.

In particular, the combined evaluation of the V/A ratio and pump efficiency, which has been scarcely addressed in the existing literature, quantifies the impact of these parameters on system performance. Hence, this study contributes to the limited body of research by presenting a detailed numerical assessment of their effects.

The remainder of this paper is organized as follows: Section 2 presents the methodology and modeling framework; Section 3 discusses the parametric results; and Section 4 summarizes the main conclusions and engineering implications.

Materials and Methods

In this section, the overall configuration of the metal hydride-based hydrogen storage system investigated in the study is described. The assumptions and boundary conditions employed for the modeling are presented, followed by a detailed formulation of the thermodynamic and exergy equations. Finally, the model validation approach is evaluated. Accordingly, the methodology has been structured not only to outline the computational procedure but also to highlight the similarities and differences of the system with real engineering applications.

System Description and Components

The system analyzed in this work is a compact hydrogen storage configuration consisting of N series-connected metal hydride reactors, a pump, temperature sensors, a coolant reservoir, and pipelines (Fig. 1) [19], [21]. The pump circulates the coolant through the reactors, removing the heat released during the absorption process and maintaining the thermal balance of the system. This configuration is consistent with the experimental multi-tube reactor designs reported in the literature [19], [21].

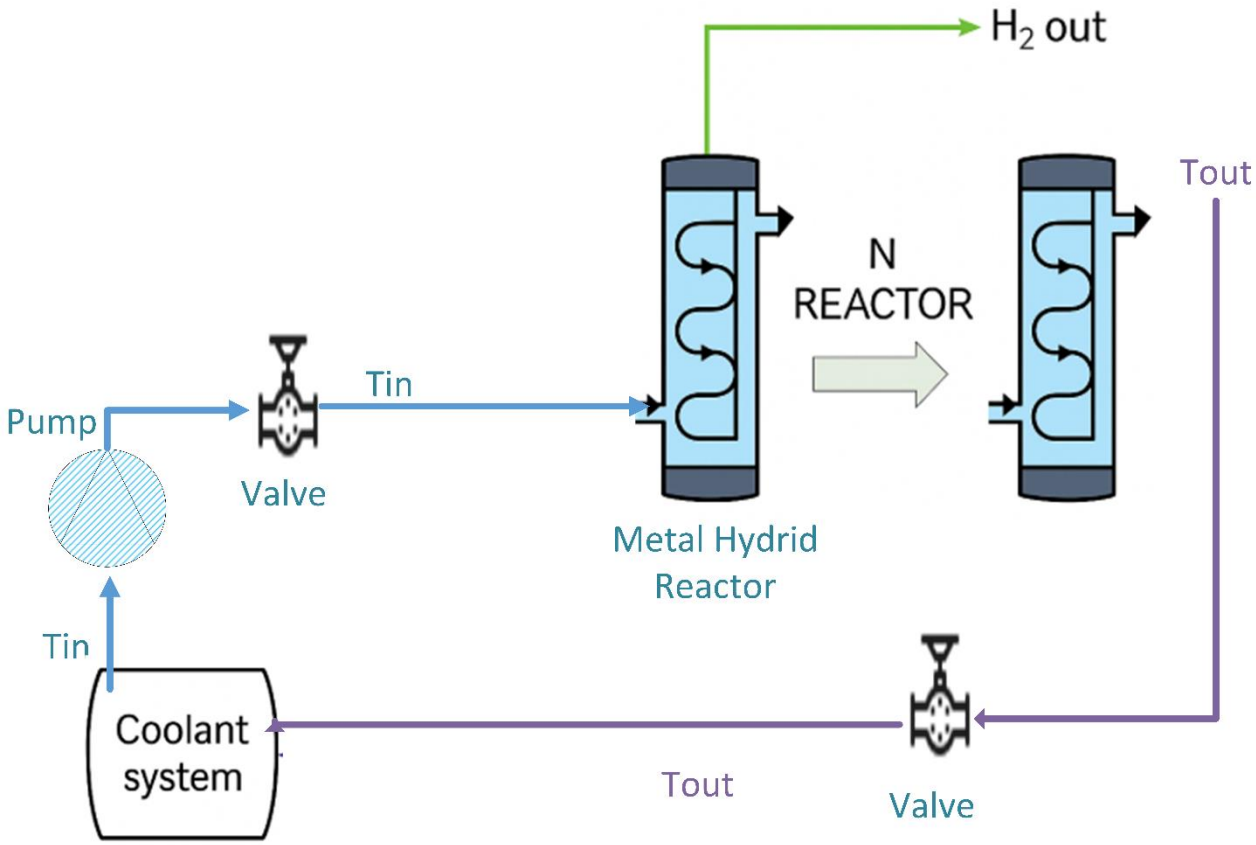

Figure 1. Schematic representation of the metal hydride-based hydrogen storage system

The model systematically investigates the influence of parameters such as ambient temperature, pump efficiency, and reactor volume-to-surface area (V/A) ratio on exergy efficiency, which are often neglected in the literature. Similar approaches have previously been conducted using CFD-based software (e.g., COMSOL, ANSYS Fluent) [22], [24], [25]; however, these studies have typically focused on a single parameter, such as tube geometry or fin configuration. In contrast, the present work addresses this gap by providing a comprehensive multivariable exergy analysis [14], [25].

Assumptions and Boundary Conditions

The main assumptions employed in the model are summarized as follows:

- The metal hydride bed was assumed to be homogeneous, and its thermophysical properties were considered constant. This simplification is consistent with literature where local thermal and mass transfer equilibrium among hydride particles is assumed [19], [25].
- The reactor shell was modeled as adiabatic, and external heat losses were neglected. This assumption is justified by studies reporting that heat losses contribute less than 2% of the total system energy in well-insulated configurations. In the exergy analysis, the ambient temperature was only varied as a reference state, and no physical heat loss to the environment was considered [21], [25].
- The ambient temperature (T_0) was initially taken as 298.15 K but was treated as a variable parameter in the sensitivity analysis to examine the dependence of exergy efficiency on environmental conditions [28].
- Water was selected as the cooling fluid and modeled using forced convection correlations [29]. The choice of water was based on its high specific heat capacity (4.18 kJ/kg·K) and low viscosity, which together maximize heat transfer efficiency inside the reactor.
- The enthalpies of absorption/desorption and the hydrogen storage capacity were adopted from literature data . These represent average values for MgH_2-based systems and were used as reference parameters for comparative evaluation [19], [21].
- The diameter of the cooling channel was assumed to be *d = 0.02 m*, ensuring a forced convection regime while avoiding transition to turbulence, in agreement with similar configurations reported in previous studies[17], [18].

These assumptions are consistent with those applied in comparable experimental and numerical investigations [19], [21], [25]. Each assumption was selected to preserve the physical integrity of the system while reducing computational complexity and ensuring an accurate representation of overall system behavior.

Thermodynamic Modeling

The modeling process was defined to preserve the physical meaning of the energy and exergy equations.

The energy requirement per reactor is expressed as follows [29]:

$$\mathrm{Q_{reactor}} = m_{MH} * \Delta\mathrm{H} * \mathrm{CH2} \quad (1)$$

where m_{MH} is the mass of the metal hydride in the reactor (kg), ΔH is the hydrogen absorption enthalpy (kJ/mol), and C_{H2} is the hydrogen storage capacity per unit mass of MH (mol/kg).

Equation (1) forms the basis of the system's heat balance and represents the change in chemical bond energy during the absorption/desorption process. The energy requirement is directly proportional to the hydrogen saturation capacity of the material [20], [21].

The total system requirement is calculated according to the number of reactors [29]:

$$E_{out} = \mathrm{N} * \mathrm{Q_{reactor}} \quad (2)$$

This equation forms the basis of scalability analysis in multi-reactor systems. While increasing the number of reactors linearly enhances the total energy capacity, it may impose certain limitations on exergy efficiency[25].In this study, it was noted that metal hydrides are not fully utilized in practical applications to their theoretical capacity. Therefore, a conversion ratio (X) was added to the storage unit used in the programming, and this ratio was chosen within the range of 0.5–0.8, typical values reported in the literature. Thus, the usable capacity of the system was modeled similarly to the charge-discharge characteristics of existing batteries.

This approach accounts for the reduction in storage capacity that occurs in practical systems due to material saturation, surface oxidation, and heat transfer limitations [19], [21], [30]. Consequently, the proposed model characterizes the energy storage effectiveness in a manner analogous to the usable charge–discharge ratio observed in electrochemical battery systems.

The governing energy equations in this section were solved through a modular computational algorithm developed in MATLAB R2021a. Each equation was solved iteratively as a function of the system's physical parameters, ensuring both numerical stability and physical consistency. The comparative results of these simulations are illustrated in Figures 2–9 [25], [31].

Heat Transfer Analysis

The heat transfer surface was modeled according to Newton's law of cooling, which establishes the relationship between the convective heat flux and the temperature difference between the surface and the surrounding fluid:

$$\mathrm{h} = \frac{(E_{out} * 1000)}{(\mathrm{A} * \Delta\mathrm{T})} \quad (3)$$

where h is the heat transfer coefficient (W/m²·K), A is the heat transfer area (m²), and ΔT is the temperature difference (K).

The heat transfer coefficient (h) was calculated using forced convection correlations and is directly dependent on the thermophysical properties of the working fluid, including specific heat capacity, density, viscosity, and thermal

conductivity [28], [29], [31]. The classical relationship between the Nusselt (Nu), Reynolds (Re), and Prandtl (Pr) numbers was employed in the correlations.

$$Nu = 0.023 * Re^{0.8} * Pr^{0.4} \quad (4)$$

This expression corresponds to the Dittus–Boelter correlation, commonly applied for estimating the convective heat transfer coefficient in turbulent flow regimes [33]. It provides an empirical relation between the Nusselt number and the Reynolds and Prandtl numbers, ensuring accurate modeling of forced convection heat transfer.

The energy carried by the coolant is given as:The energy carried by the coolant is expressed as:

$$E_{\text{in}} = \dot{m} * cp * (\text{T}_{in} - \text{T}_{out}) * \text{t} \quad (4)$$

where $\dot{m}$ is the mass flow rate of the coolant (kg/s), cp, is the specific heat capacity of the coolant (kJ/kg·K), T_{in} is the inlet temperature (K), and T_{out} is the outlet temperature (K), and t is the cycle time of a reactor (s).

The thermal adequacy of the system was assessed by comparing Ein and Eout. When Ein<Eout , the system is at risk of overheating, whereas for Ein>Eout, cooling is safe but may lead to reduced efficiency.

In this study, in order to better reflect the impact of the heat transfer coefficient (h) on exergy efficiency, the cycle time (t) was assumed to be inversely proportional to hhh (t∝1/h). As h increases, the cycle time decreases, the energy transferred per unit time through the Ein equation rises, and the exergy efficiency of the system improves. This relation represents a simplified model reflecting the trend reported in the literature [19], [21], although in real systems it may vary depending on material properties, reactor geometry, and fluid conditions.

Pump Power Calculation

The power consumed by the pump is expressed as [33]:

$$\text{W}_{\text{pump}} = \frac{\dot{\text{m}} \cdot \Delta\text{P}}{\eta_{\text{pump}} * \rho} \quad (5)$$

where η_{pump} is the pump efficiency, and ρ is the fluid density.

Exergy Analysis

The inlet exergy of the coolant is given as [34]:

$$Exin = \dot{\text{m}} * cp * \left[(\text{T}_{out} - \text{T}_o) - (\text{T}_{in} - \text{T}_o) - \text{T}_o * \ln\left[\frac{\text{T}_{in}}{\text{T}_o}\right]\right] \quad (6)$$

where $\dot{m}$ is the mass flow rate (kg/s), T is the inlet temperature of the coolant (K), T_0 is the ambient temperature (K), and cp is the specific heat capacity at constant pressure (kJ/kg·K).

The useful exergy is calculated as:

$$E_{\text{x,useful}} = \text{Q}_{\text{total}} * \left(1 - \left(\frac{\text{T0}}{\text{Tavg}}\right)\right) \quad (7)$$

With

$$\text{Tavg} = \frac{(\text{Tin} + \text{Tout})}{2} \quad (8)$$

This formulation defines the portion of thermal energy that can be converted into useful work, with reference to the ambient temperature T_0. In the present analysis, the ambient temperature was taken as T_0= 298.15 K (25 °C) as a baseline, but was also varied as a parameter in the Second Law analysis to investigate its influence on exergy efficiency.

The exergy efficiency of the system is defined as the ratio of the net useful work obtained to the total input exergy. In this study, the net work output (W_{net}), the pump power (W_{pump}), and the input exergy supplied by the coolant (Ex_{in}) were used to calculate the exergy efficiency [28]:

$$\text{n}_{\text{ex}} = \frac{E_{\text{x,useful}}}{E_{\text{x.in}} + W_{pump}} \quad (9)$$

The total exergy destruction in the system was determined to evaluate the Second Law losses, using the following expression[28], [34];

$$\text{Ex}_{\text{D}} = E_{\text{x.in}} - E_{\text{x,useful}} \quad (10)$$

Where Ex_{in} is the total inlet exergy carried by the coolant (kJ/s), and Ex_{useful} is the exergy amount effectively converted into useful output (kJ/s).

These analyses allow the energy and exergy performance of the system to be evaluated under different operating scenarios.

Error Analysis

An error analysis was conducted to evaluate the consistency of the model outputs with the experimental data reported in the literature. In this context, the root mean square error (RMSE) and the relative error (Δ%) were calculated as follows:

$$\text{RMSE} = \sqrt{\frac{1}{n}\sum_{i=1}^{n}\left(\eta_{ex,\text{i}}^{model} - \eta_{ex,\text{i}}^{exp}\right)} \quad (11)$$

$$\%\Delta = \frac{\eta_{ex}^{model} - \eta_{ex}^{exp}}{\eta_{exp}} * 100 \quad (12)$$

where η_{ex} refers to the exergy efficiency, with superscripts "model" and "exp" denoting the values obtained from the model and experimental data, respectively. RMSE indicates the overall level of agreement, while the relative error highlights local deviations.

The reliability of the model was assessed in the Results section through an error analysis based on RMSE and relative error, using literature data as reference.

Parametric Analyses

The engineering and thermodynamic parameters used in this study were determined based on a magnesium hydride (MgH_2)–based metal hydride reactor system. Each parameter employed in the model was directly linked to the assumptions defined in Sections 2.2–2.4 and solved using a computational algorithm developed in MATLAB R2021a.

Table 1 presents the fixed assumptions, material properties, and system boundary conditions adopted from the literature. These parameters were selected within the ranges commonly reported in previous studies to ensure both scientific validity and comparability of the model results.

The selection of parameter ranges followed the recommendations of recent works [19], [21], [32], thereby maintaining consistency with established experimental and numerical data. The pump efficiency (η_{pump}) was fixed at 0.7 in the baseline analysis, consistent with the 0.6–0.8 range reported by [25], [29]. To evaluate the system's sensitivity to pump performance, η_{pump} was varied between 0.6 and 0.8, and the resulting trends are illustrated in Figure 5.

The absorption enthalpy of MgH_2, approximately −75 kJ mol^{-1} H_2, is a critical parameter governing the system's heat requirement and forms the thermodynamic basis for both the energy and exergy analyses. This value was used to calculate the temperature-dependent components of the energy balance and exergy efficiency, ensuring physical consistency with the literature.

Table 1. Thermodynamic parameters and assumptions for the MgH_2-based system

Parameter	Symbol	Value	Unit	Description	Source/Note
Mass of metal hydride (per reactor)	m_{MH}	2	kg	Assumed constant per reactor	Assumption
Hydrogen absorption enthalpy	ΔH	−75	kJ/mol H_2	Typical reaction enthalpy for MgH_2	[32]
H_2 storage capacity	C_{H2}	7.6 wt% (≈ 38)	wt% / mol·kg^{-1}	Maximum theoretical H_2 capacity of MgH_2; wt% converted to mol/kg	[32]
Specific heat (water)	cp	4.18	kJ/kg·K	Water used as coolant	[29]
Fluid density (water)	ρ	997	kg/m^3	Assumed constant at 25–30 °C	[29]
Coolant outlet temperature	T_{out}	333.15	K	Varied in the range 50–70 °C	Assumption
Coolant inlet temperature	T_{in}	313.15	K	Assumed as 40 °C	Assumption
Ambient temperature	T_0	298.15	K	Reference temperature (25 °C)	Assumption
Heat transfer coefficient	h	2000	W/m^2·K	Average value for MH heat transfer analyses	[31]
Pump efficiency	η_{pump}	0.7	–	Typical efficiency range in practical systems	Assumption
Pump pressure difference	ΔP	2×10^5	Pa	Typical value for compact systems	Assumption
Average flow velocity	v	1.5	m/s	In-pipe liquid velocity	Assumption
Chemical formula of MH	–	MgH_2	–	Active storage material	Assumption
Pump efficiency	ηpump	0.5	–	Assumed baseline value for pump performance	Assumption

While most studies in the literature focus on single-parameter or limited-variable analyses [19], [21], this study adopts a multi-parameter approach. Parameters including reactor number, inlet temperature, mass flow rate, pump efficiency, ambient temperature, heat transfer coefficient, and the volume-to-surface (V/A) ratio were systematically analyzed from an exergy perspective. This holistic approach not only examines the energy balance but also provides a multidimensional evaluation of Second Law (exergy) efficiency, which is rarely addressed in the literature [22], [24], [25].

Efficiency with Respect to Reactor Number

In metal hydride (MH)-based hydrogen storage systems, the number of reactors is a key design parameter that directly affects the energy and exergy performance.Increasing the number of reactors enhances both the total storage capacity and the available energy output of the system, without

causing a significant change in pump power requirements. This indicates that multi-reactor configurations can offer more sustainable and efficient solutions, particularly for industrial-scale applications. Table 2 presents the MgH_2-based model results for different reactor numbers and allows for comparison with previous studies in the literature. In particular, parameters such as energy output (Eout), pump power (Wpump), and exergy efficiency (ηex) are analyzed to describe the performance variations in detail. Accordingly, the performance improvements achieved with higher reactor numbers can be clearly observed.

Table 2. System performance as a function of reactor number and comparison with literature

System / Study	Reactor Number (N)	Total MH Mass (kg)	Hydrogen Storage (g)	E_{out}	W_{pump} (kJ/s)	η_{ex} (%)
This Study (MgH_2, modeling)	2	10	–	31.67	0.286	21.5
This Study (MgH_2, modeling)	4	20	–	63.33	0.286	43.2
This Study (MgH_2, modeling)	6	30	–	95.00	0.286	64.9
Jana & Muthukumar (2023, TBR) [19]	19	26.5 ($La_{0.8}Ce_{0.2}Ni_5$)	369.1	0.8–1.7	–	58–64
Parashar & Muthukumar (2024, multi-tube compact) [35]	Multi-tube compact	Ti–Zr–Mn–V–Fe alloy	164.3(abs) / 153.6(des)	0.095	–	82.3

The results in Table 2 indicate that the energy output increases almost linearly with the number of reactors, while the exergy efficiency shows a notable improvement. For instance, the exergy efficiency (ηex) increases from 21.5% in the two-reactor system to 64.9% in the six-reactor configuration. The experimental study by Jana and Muthukumar (2023) [19], along with the compact design proposed by Parashar and Muthukumar (2024) [21], demonstrates that high efficiency values can be achieved using alternative alloys and configurations. In this context, although the model results are lower than the literature values at low reactor numbers, they gradually converge with experimental data as the reactor number increases. This trend indicates that the model is scalable.

To further evaluate the model's reliability, Table 2a presents an error analysis in comparison with the literature data reported by Jana (2023) [19], Parashar (2024) [21], and Eisapour (2025) [36]. The root mean square error (RMSE) and relative error (%) values are reported to quantify the level of agreement.

Table 2a. Error analysis of model results compared to literature data (RMSE and relative error)

η_{ex}	$\eta_{Jana2023}$	RMSE (Jana)	Rel. Error (Jana, %)	$\eta_{Parashar2024}$	RMSE (Parashar)	Rel. Error (Parashar, %)	$\eta_{Eisapour2025}$	RMSE (Eisapour)	Rel. Error (Eisapour, %)
17.67	61.0	43.33	−71.04	82.3	64.63	−78.53	31.5	13.83	−43.92
35.33	61.0	25.67	−42.08	82.3	46.97	−57.07	31.5	3.83	12.17
53.00	61.0	8.00	−13.12	82.3	29.30	−35.60	31.5	21.50	68.25

The results in Table 2a indicate that the discrepancies between the model and literature data decrease with an increasing number of reactors. For instance, the relative error with Jana (2023) [19] decreases from −71.04% at two reactors to −13.12% at six reactors. Likewise, when compared with Parashar (2024) [21], the error decreases from −78.53% to −35.60%. The comparison with Eisapour (2025) [36] shows smaller deviations, confirming that the model converges well with literature trends for specific parameters. Therefore, Table 2a demonstrates the model's scalability potential and its ability to align with literature data.

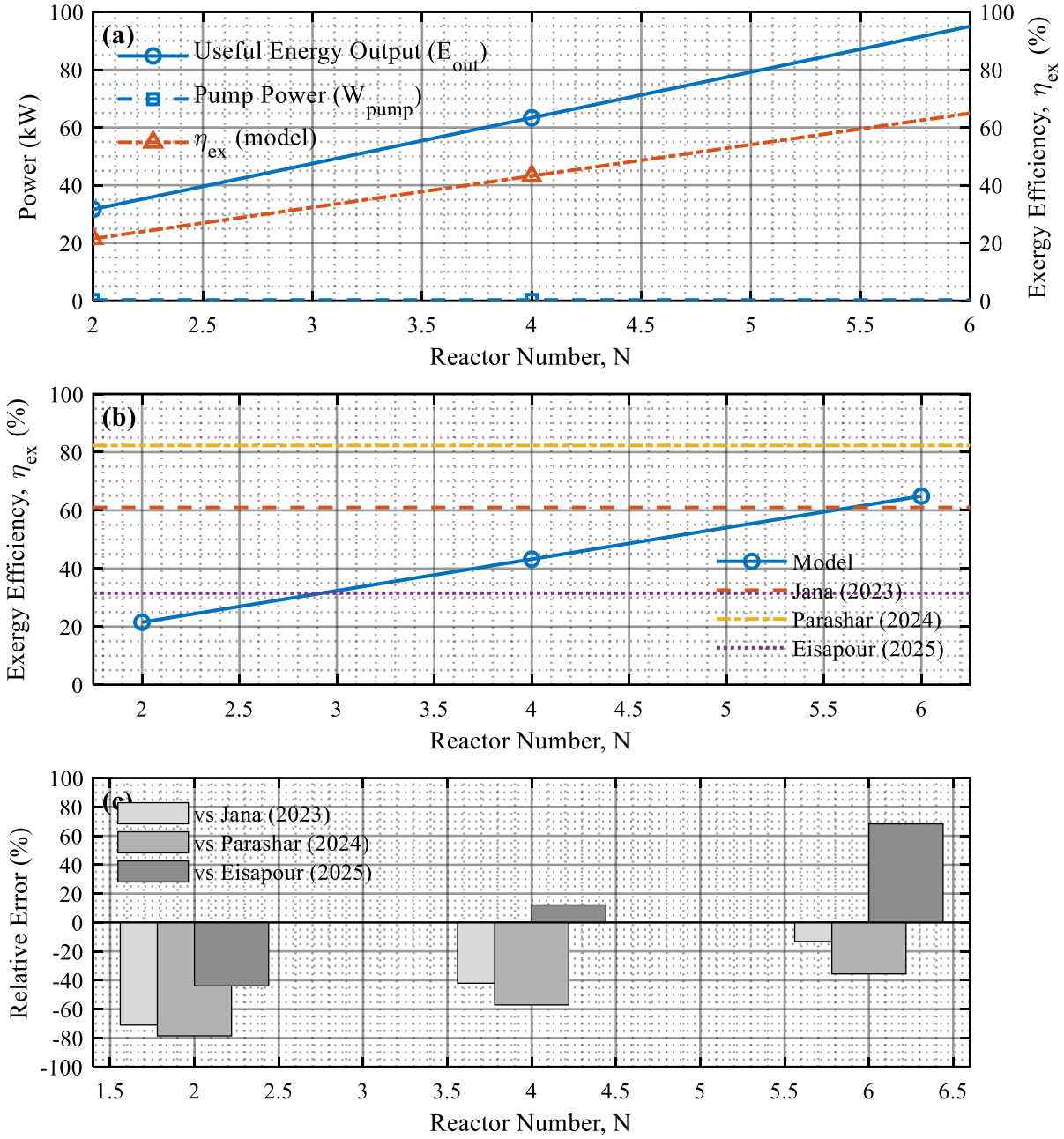

Figure 2. Effect of reactor number on system performance

Figure 2a compares the useful exergy (Exuseful), exergy efficiency (ηex), and pump power (Wpump). As the number of reactors increases, both useful exergy and efficiency increase steadily, while pump power remains almost constant. Figure 2b presents a comparison between the model results and literature data (Jana 2023 [19]; Parashar 2024 [35]; Eisapour 2025 [36]. The model shows closer agreement with literature values as the reactor number increases. Figure 2c depicts the relative error analysis, where deviations are significant at low reactor numbers but decrease markedly at higher ones. These results confirm that the model is scalable and highly consistent with literature data for multi-reactor systems.

Effect of Outlet Temperature

In MH reactors, the outlet temperature is a key factor affecting the system's exergy performance. Hydrogen absorption and desorption are directly dependent on temperature; therefore, variations in outlet temperature strongly impact both available exergy and system efficiency. Analyzing model results at different outlet temperatures (50–70 °C) is essential to identify the optimum operating range. Table 3 presents the results for exergy input (Exin), useful exergy (Exuseful), pump power (Wpump), and exergy efficiency (ηex). It also lists comparative data from Askri (2019) [37], Alqahtani (2024) [38], and Ayub (2020) [39], enabling direct comparison with previous experimental and theoretical studies.

Table 3. Effect of outlet temperature and comparison with literature

T_{out}(°C)	Ex_{in}(kJ/s)	W_{pump}(kJ/s)	η_{ex}(%)
50	2.6166	0.4	65.99
60	6.4236	0.4	35.90
70	11.3507	0.4	24.64
Askri(2019) [37], ~60 °C	–	–	30–40
Alqahtani(2024)[42], 50–70 °C	–	–	32–38
Ayub(2020)[39], 70–80 °C	–	–	35–40

Table 3 shows that exergy efficiency decreases notably as the outlet temperature increases. Efficiency drops from 65.99% at 50 °C to 24.64% at 70 °C. This decline results from slower absorption kinetics and higher heat transfer demand at elevated temperatures. Reported literature values range between 30–40% around 60 °C (Askri, 2019) [37], 32–38% within 50–70 °C (Alqahtani, 2024) [38], and 35–40% for 70–80 °C (Ayub, 2020) [39]. The model results align well with these studies, particularly in the 50–60 °C range. At 70 °C, the efficiency is slightly lower due to absorption limitations. Figure 3 presents the combined influence of outlet temperature on overall system performance.

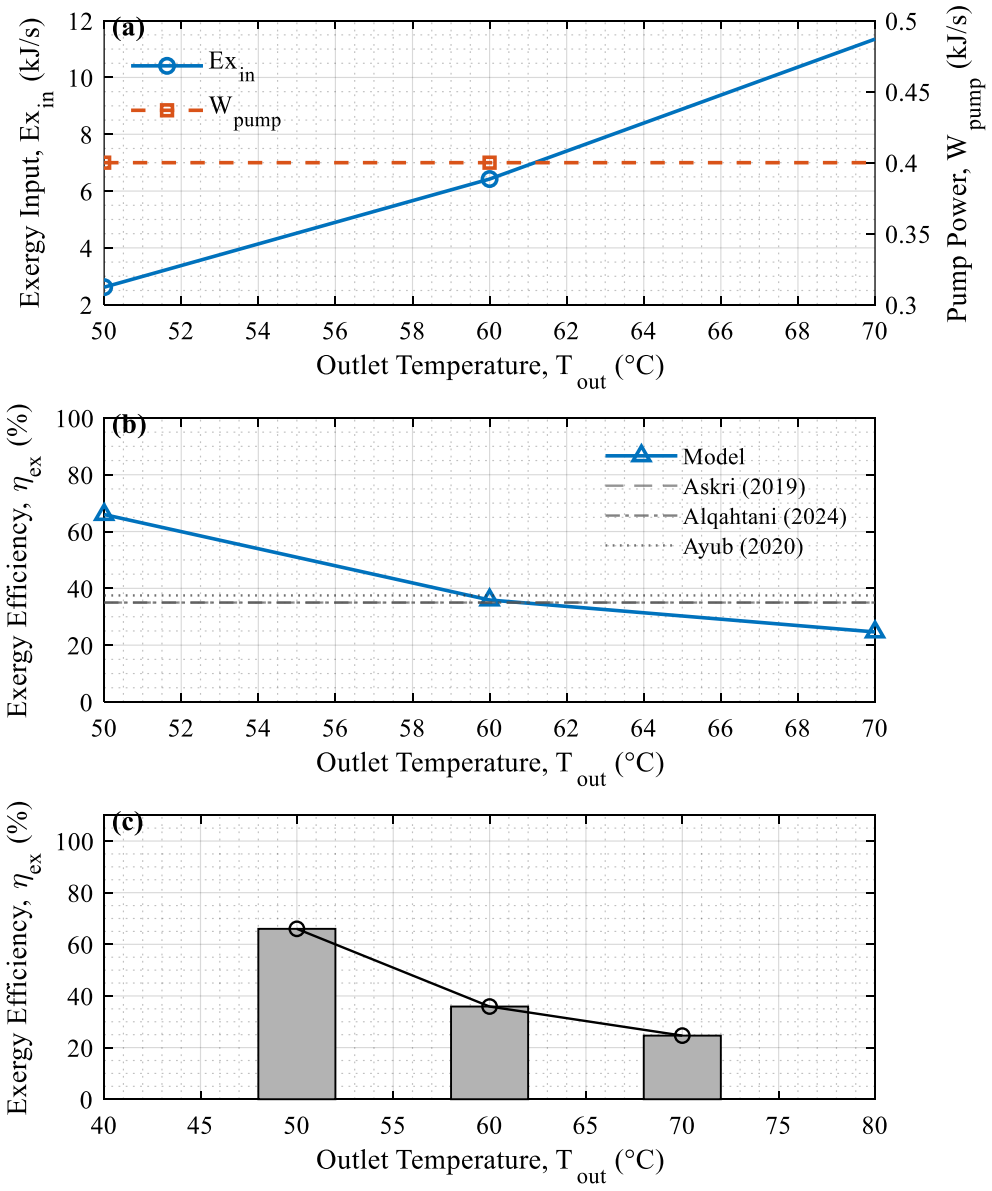

Figure 3. Variation of reactor number and exergy efficiency with outlet temperature

Figure 3 shows that the optimum absorption temperature lies within the 50–60 °C range. Beyond this range, the system's exergy performance declines noticeably. Figure 3(a) presents the relationship between exergy input (Ex_in) and pump power (W_pump) as outlet temperature increases. Exergy input rises with temperature, while pump power remains constant, reflecting greater energy demand at higher temperatures. Figure 3(b) compares the model results with previous studies by Askri (2019) [37], Alqahtani (2024) [38], and Ayub (2020) [39]. The model aligns well with literature data at lower temperatures, but efficiency deviations appear at higher temperatures due to limited absorption kinetics. Figure 3(c) shows the variation of exergy efficiency with reactor number. Efficiency improves as the reactor number increases; however, this trend weakens at higher temperatures, particularly at 70 °C.

In MH-based hydrogen storage systems, the coolant mass flow rate is a key parameter influencing heat transfer and overall system performance. As the flow rate increases, more fluid passes over the heat transfer surface, which enhances heat removal during absorption. However, the higher flow rate also increases pump power demand and reduces exergy efficiency. Evaluating the system under different mass flow rates is therefore essential to determine the optimum operating range. Table 4 presents the effect of mass flow rate variation (0.5–1.5 kg/s) on system parameters. In this study, the mass flow rate (ṁ), volumetric flow rate (V), pump power (Wpump), exergy input (Exin), useful exergy (Exuseful), and exergy efficiency (ηex) were calculated. These parameters provide a quantitative basis for assessing how flow rate changes affect the system's exergy performance.

Effect of Mass Flow Rate

Table 4. Effect of mass flow rate

$\dot{m}$(kg/s)	V (m³/s)	W_{pump} (kJ/s)	Ex_{in} (kJ/s)	Ex_{useful} (kJ/s)	η_{ex} (%)
0.5	0.0005015	0.2006	5.6924	2.895	49.13
1.0	0.001003	0.4012	11.385	2.895	24.56
1.5	0.0015045	0.6018	17.077	2.895	16.38

Table 4 shows that exergy efficiency decreases notably as the mass flow rate increases. For example, efficiency is 49.13% at 0.5 kg/s and drops to 16.38% at 1.5 kg/s. This decline results from the higher pump power required at greater flow rates. Similar trends are reported in the literature. Nyamsi (2021) [27] and Krane (2022) [40] observed that increasing the flow rate beyond a threshold enhances heat transfer but lowers exergy efficiency due to higher energy losses. Accordingly, the model results in Table 4 align well with the literature and indicate that the optimum flow rate lies within the low-to-medium range.

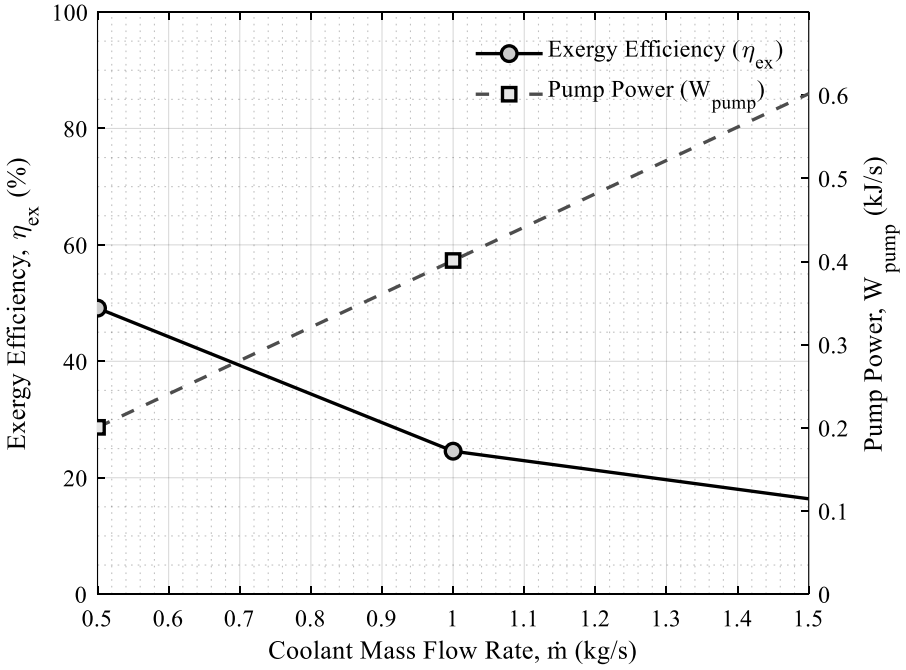

Figure 4. Effect of coolant mass flow rate on exergy efficiency

Figure 4 shows that exergy efficiency decreases as the flow rate increases. At lower flow rates (0.5 kg/s), higher efficiencies are obtained, but efficiency declines sharply at higher flow rates. This behavior agrees with literature findings. Krane (2022) [40] reported that higher flow rates improve heat transfer but lower efficiency due to greater pump power demand. Figure 4 therefore provides clear evidence for the optimum mass flow rate and confirms that the model aligns with literature trends.

Effect of Pump Efficiency on System Performance

Pump efficiency is a key parameter that indirectly influences the exergy performance of hydrogen storage systems. Higher pump efficiency increases the effective power delivered to the system and reduces pump-related losses. Variations in efficiency therefore play an important role in assessing overall exergy performance. To examine this effect, calculations were performed for different ηpump values. The related parameters—pump power (Wpump), exergy input (Exin), useful exergy (Exuseful), exergy destruction (ExD), and exergy efficiency (ηex)—were calculated. The summarized results are presented in Table 5.

Table 5. Effect of pump efficiency on exergy and power

η_{pump}	Wpump (kJ/s)	Ex_{in} (kJ/s)	Ex_{useful} (kJ/s)	Ex_D (kJ/s)	η_{ex} (%)
0.6	0.3333	11.351	2.895	8.4556	24.78
0.7	0.2857	11.351	2.895	8.4556	24.88
0.8	0.2500	11.351	2.895	8.4556	24.96

Table 5 shows that increasing pump efficiency from 60% to 80% reduces pump power consumption from 0.3333 kJ/s to 0.2500 kJ/s. In parallel, exergy efficiency rises slightly from 24.78% to 24.96%. These results indicate that the direct influence of pump efficiency on overall system performance is limited but positive. Literature studies report similar trends, showing that auxiliary components such as pumps make a small yet meaningful contribution to the performance of MH-based storage systems [27], [40]. Therefore, pump selection should account for both energy consumption and its effect on overall exergy efficiency.

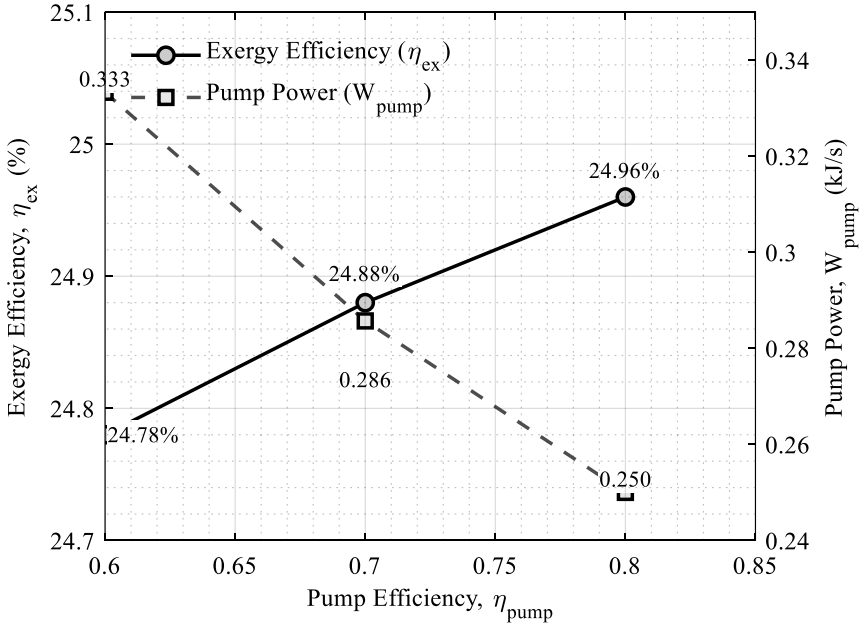

Figure 5. Effect of pump efficiency on exergy efficiency

Figure 5 shows that exergy efficiency increases slightly but linearly as pump efficiency improves. At 60% pump efficiency, exergy efficiency is about 24.78%, and it rises to 24.96% at 80%. This small change helps reduce energy losses during long-term operation. Krane (2022) [40] and Nyamsi (2021) [27] also reported that pumps and other auxiliary components have an indirect but notable effect on overall energy and exergy performance. These findings confirm that high-efficiency pumps are crucial for sustainable hydrogen storage systems.

Effect of Ambient Temperature on Exergy

Ambient temperature (T_0) is a key environmental parameter influencing the performance of thermodynamic processes. In exergy analysis, it defines the reference condition and serves as a basis for calculating exergy input, destruction, and efficiency. Three scenarios were analyzed in this study with ambient temperatures of 20 °C, 25 °C, and 30 °C. For each case, the exergy input (Exin), exergy destruction (ExD), useful exergy (Exuseful), pump power (Wpump), and exergy efficiency (ηex) were computed. The summarized results are presented in Table 6.

Table 6. Effect of ambient temperature on exergy efficiency

T_0 (°C)	Ex_{in} (kJ/s)	Ex_D (kJ/s)	Ex_{useful} (kJ/s)	W_{pump} (kJ/s)	η_{ex} (%)
20	13.257	9.8794	3.3775	0.2857	24.94
25	11.351	8.4556	2.895	0.2857	24.88
30	9.4444	7.0318	2.4125	0.2857	24.79

Table 6 shows that a rise in ambient temperature slightly decreases the system's exergy performance. For instance, exergy efficiency declines from 24.94% at 20 °C to 24.79% at 30 °C. This decline occurs because higher ambient temperatures reduce the exergy gradient with the surroundings and lower the amount of useful exergy. Similar patterns are reported in the literature. Nyamsi (2021) [27] and Krane (2021) [41] observed that changes in ambient conditions alter the system's thermodynamic potential and cause small efficiency variations. These results emphasize the need to consider ambient temperature in long-term operational analyses.

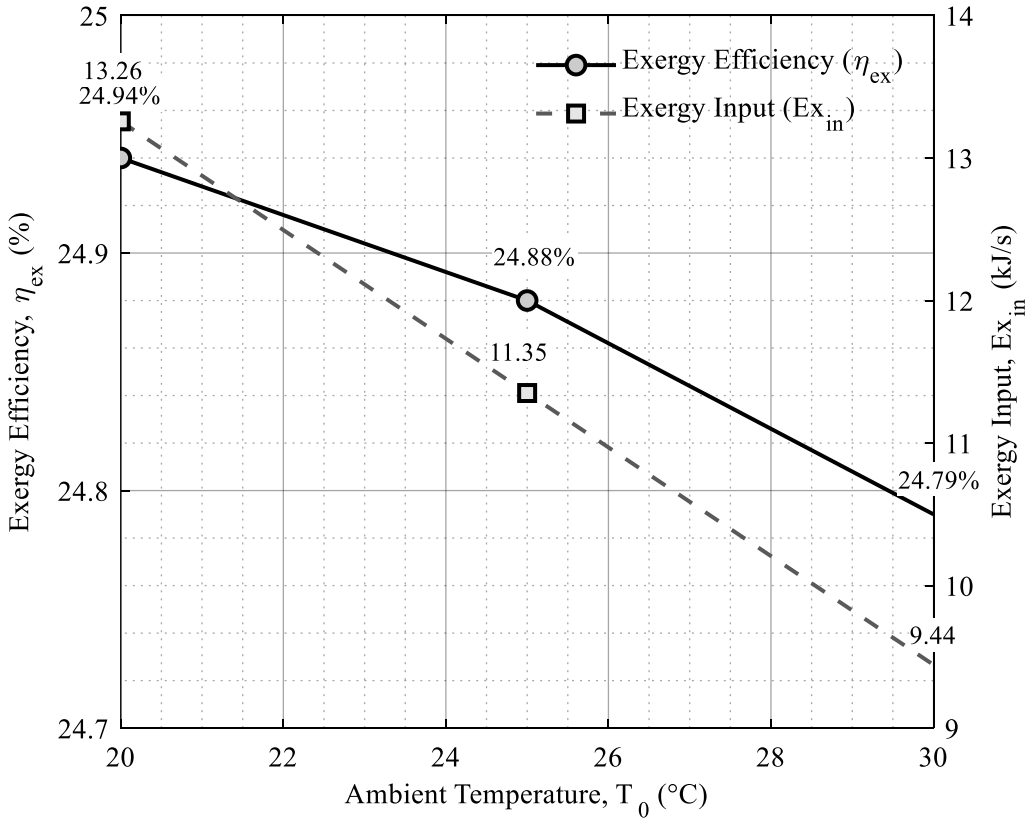

Figure 6. Effect of ambient temperature on exergy efficiency

Figure 6 shows that exergy efficiency decreases linearly as ambient temperature increases. The system exhibits higher exergy potential at lower ambient temperatures, but this potential declines under warmer conditions. Krane (2021) [41] noted that environmental factors, especially fluid inlet and ambient temperatures, strongly affect system

performance. Likewise, Nyamsi (2021) [27] found that environmental parameters cause small changes in both energy and exergy efficiency. These findings confirm that the model results align with the literature and emphasize the need to consider ambient temperature in design optimization.

Effect of Heat Transfer Coefficient (h) on System Performance

The absorption process is the main mechanism that enables hydrogen storage in MH reactors, where an exothermic reaction occurs. If the released heat is not removed effectively, the absorption rate drops and system performance declines. The heat transfer coefficient (h) is therefore a key parameter influencing efficiency during absorption. For different h values, total heat transfer (Qtotal), exergy input (Exin), useful exergy (Exuseful), pump power (Wpump), and exergy efficiency (ηex) were computed. The results are presented in Table 7.

Table 7. Effect of heat transfer coefficient on system performance

h (W/m²·K)	Qtotal (kJ/s)	Exin (kJ/s)	Exuseful (kJ/s)	Wpump (kJ/s)	η_{ex} (%)
1000	31.667	11.351	2.895	0.400	24.64
2000	63.333	11.351	5.790	0.400	49.27
3000	95.000	11.351	8.685	0.400	73.91

Table 7 shows that a higher heat transfer coefficient (h) during absorption directly improves system performance. At h = 1000 W/m²·K, exergy efficiency is 24.64%, and it rises to 73.91% at h = 3000 W/m²·K. This improvement indicates that larger h values enable more effective heat removal from the reactor and accelerate the absorption process, leading to higher exergy efficiency. Literature studies confirm this trend. Jana (2023) [19] found that greater surface areas in tube bundle reactors shorten absorption time. Parashar (2024) [21], [35] reported that enhanced heat transfer in compact multi-tube reactors increases absorption capacity. Likewise, Eisapour (2025) [36] showed that PCM-integrated conical heat exchangers reduce charging times by 30–69% during absorption. These findings confirm that the model results agree well with the literature.

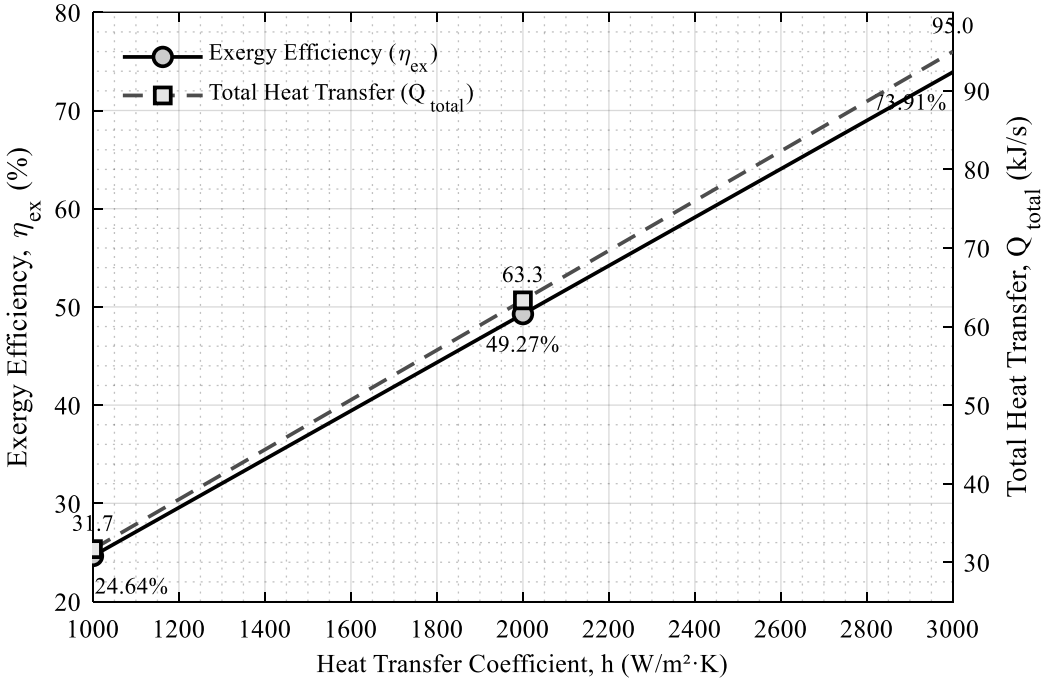

Figure 7. Effect of heat transfer coefficient on exergy efficiency

Figure 7 shows that exergy efficiency increases linearly with the heat transfer coefficient (h) during absorption. At low h values, poor heat removal restricts the absorption rate. At higher h values, effective heat dissipation allows faster and more efficient hydrogen storage. Literature studies confirm this trend. Jana (2023) [19], Parashar & Muthukumar (2024) [21], [35], and Eisapour (2025) [36] found that improving the heat transfer coefficient reduces absorption time and increases storage capacity, leading to higher efficiency. Reactor designs that achieve high h values—such as multi-tube configurations, conical heat exchangers, and PCM-integrated systems—are therefore essential for improved performance.

Effect of Hydrogen Loading Capacity (C_{H2}) on System Performance

In MH-based hydrogen storage systems, the hydrogen loading capacity of the material (CH_2) is a key parameter influencing storage density and overall exergy performance. Materials with higher hydrogen capacity can store more hydrogen and thus yield greater useful exergy, leading to improved system efficiency. Three hydrogen loading capacities—20, 30, and 40 mol/kg—were analyzed in this study. For each case, the exergy input (Exin), useful exergy (Exuseful), pump power (Wpump), exergy destruction (ExD), and exergy efficiency (ηex) were computed. The summarized results are presented in Table 8.

Table 8. Effect of hydrogen loading capacity on exergy efficiency

C_{H2} (mol/kg)	Ex_{in} (kJ/s)	Ex_{useful} (kJ/s)	W_{pump} (kJ/s)	Ex_D (kJ/s)	η_{ex} (%)
20	11.351	0.762	0.286	10.589	6.55
30	11.351	1.143	0.286	10.208	9.82
40	11.351	1.524	0.286	9.827	13.09

Table 8 shows that higher hydrogen capacity significantly enhances system performance. For instance, exergy efficiency (ηex) is 6.55% at CH_2 = 20 mol/kg and increases to 13.09% at CH_2 = 40 mol/kg. This improvement occurs because storing more hydrogen raises useful exergy and lowers exergy destruction. Literature studies confirm this trend, showing that MH materials with greater hydrogen capacity lead to higher efficiency and improved energy conversion [19], [21], [35], [36]. These results confirm that hydrogen capacity is a key factor in material selection.

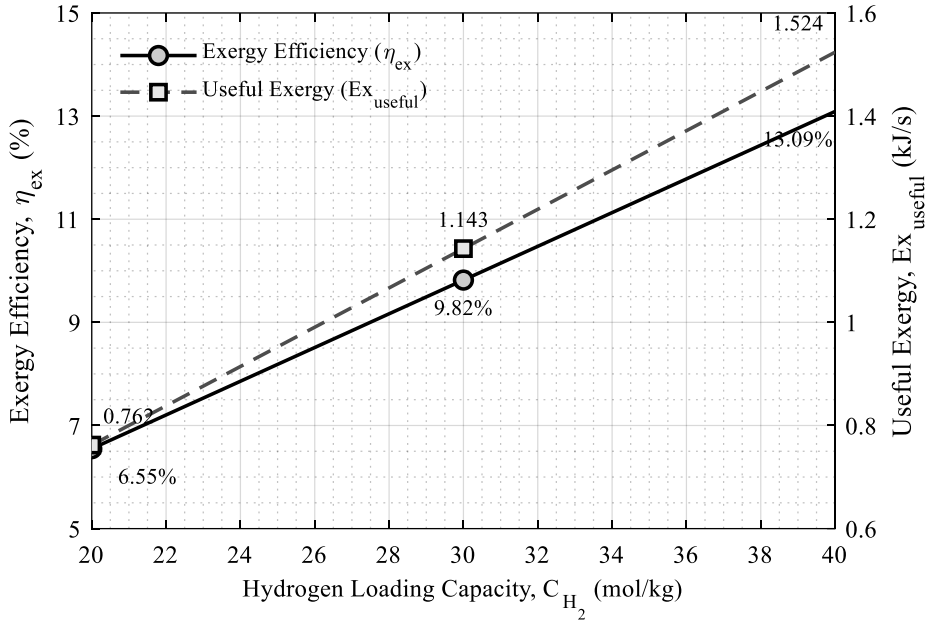

Figure 8. Variation of exergy efficiency with hydrogen loading capacity

Figure 8 shows a nearly linear relationship between hydrogen capacity and exergy efficiency. As capacity increases from 20 mol/kg to 40 mol/kg, efficiency almost doubles. This trend indicates that materials with higher capacities store more hydrogen and use energy more effectively during absorption. Similar results are reported in the literature. Jana (2023) [19] highlighted the importance of high capacity in tube bundle reactors. Parashar (2024) [21], [35] observed similar behavior in multi-tube compact reactors, while Eisapour (2025) [36] found improved charge–discharge efficiency in PCM-integrated systems. Therefore, increasing hydrogen capacity is a critical factor for system design, supported by both the model and literature evidence.

Effect of Reactor Volume-to-Surface Area (V/A) Ratio on Exergy Performance

The volume-to-surface area (V/A) ratio is a key design parameter in MH reactors because it affects heat transfer characteristics. A lower V/A ratio provides a larger surface area for heat exchange and enables faster removal of heat during absorption. In contrast, a higher V/A ratio restricts heat transfer and reduces overall system performance. In this study, the influence of the V/A ratio on exergy performance was analyzed. For V/A ratios of 0.05, 0.075, and 0.10 m, exergy input (Exin), useful exergy (Exuseful), pump power (Wpump), and exergy efficiency (ηex) were computed. The summarized results are presented in Table 9.

Table 9. Effect of V/A ratio on exergy efficiency

V/A Ratio (m)	Ex_{in} (kJ/s)	Ex_{useful} (kJ/s)	W_{pump} (kJ/s)	η_{ex} (%)
0.05	11.351	0.274	0.400	2.33
0.075	11.351	0.183	0.400	1.56
0.10	11.351	0.137	0.400	1.17

Table 9 shows that exergy efficiency decreases significantly as the V/A ratio increases. At V/A = 0.05 m, the exergy efficiency (ηex) is 2.33%, but it falls to 1.17% at V/A = 0.10 m. This reduction occurs because a smaller surface area limits heat dissipation and slows hydrogen storage kinetics. Literature studies confirm this trend. Lower V/A ratios enhance heat transfer and increase overall efficiency, while higher ratios lead to noticeable performance losses [19],[21],[35],[36]. These results emphasize the need to optimize the V/A ratio during reactor design.

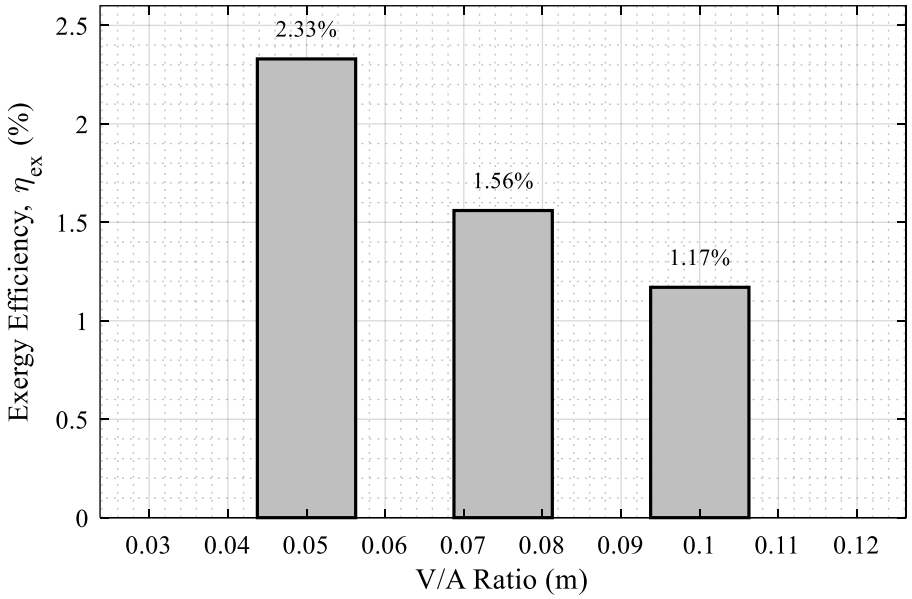

Figure 9. Variation of exergy efficiency with V/A ratio

Figure 9 shows that exergy efficiency decreases as the V/A ratio increases during absorption. Lower ratios provide a larger surface area for heat transfer and enable faster absorption. In contrast, higher ratios restrict heat dissipation and lower overall efficiency. Similar findings are reported in the literature. Jana (2023) [19] observed this effect in tube bundle reactors, Parashar (2024) [35] noted it in multi-tube compact designs, and Eisapour (2025) [36] confirmed it in PCM-integrated systems. These results verify that the model outcomes align well with literature trends.

Discussion

The multi-parametric exergy analysis conducted in this study provides a comprehensive evaluation of MgH_2-based metal hydride systems, extending beyond the single-variable approaches commonly found in the literature. The results reveal that both energy and exergy performances are highly sensitive to multiple engineering parameters, including reactor number, outlet temperature, mass flow rate, pump efficiency, ambient temperature, heat transfer coefficient, hydrogen capacity, and the reactor's volume-to-surface (V/A) ratio.

The findings related to the number of reactors are consistent with the trends reported by Jana (2023) [19] and Parashar (2024) [35], confirming that an increased number of reactors leads to a nearly linear improvement in exergy efficiency, particularly in large-scale configurations. This demonstrates the scalability potential of the proposed model. Regarding outlet temperature, the optimum absorption range was determined to be between 50 °C and 60 °C, which agrees well with the thermal equilibrium ranges reported by Askri (2019) [37] and Alqahtani (2024) [42].

The analysis of mass flow rate showed that exergy efficiency decreases as flow rate increases, mainly due to

the dominant effect of pump power consumption at higher flow conditions. This observation is in strong agreement with the concept of an "optimum flow rate window" highlighted by Krane (2022) [40] and Nyamsi (2021) [27]. Although the variation of pump efficiency (η_{pump}) did not produce large numerical changes, its indirect influence on the overall energy quality was evident. This result supports previous studies emphasizing that the efficiency of auxiliary components, such as pumps, can have a limited but meaningful impact on overall system performance.

The results related to the heat transfer coefficient strongly support the trend reported by Jana (2023) [19], Parashar (2024) [35], and Eisapour (2025) [36], indicating that higher *h* values significantly enhance the absorption rate. Notably, the exergy efficiency of 73.91% achieved at h = 3000 W/m²·K demonstrates that improving the system's heat management capability can substantially increase overall performance. Similarly, the improvements obtained by increasing hydrogen storage capacity and reducing the V/A ratio are consistent with the studies of Parashar (2024) [35] and Eisapour (2025) [36], which emphasize the importance of larger surface areas and higher storage densities in achieving superior system efficiency.

Overall, the model results exhibit strong consistency with the literature, while minor discrepancies can be attributed to differences in material composition (e.g., MgH_2 versus $LaNi_5$ or Ti–Zr alloys), temperature regimes, and heat transfer conditions. These differences do not undermine the model's validity; rather, they highlight its robustness and adaptability under varying operational scenarios.

This study represents one of the first comprehensive models to analyze the multi-dimensional interaction between energy and exergy parameters in MgH_2-based systems. It quantitatively captures the combined influence of interdependent variables, providing an integrated framework that has been largely overlooked in previous research.

In conclusion, the multi-parametric analysis clearly demonstrates that system performance must be evaluated through the coupled interaction of all governing variables. The findings not only confirm the existing trends in the literature but also yield directly applicable engineering insights for design optimization. Consequently, this work establishes the analytical foundation for the results and recommendations presented in the following section.

Conclusions and Recommendations

A comprehensive energy and exergy analysis was carried out for a magnesium hydride (MgH_2)–based metal hydride (MH) hydrogen storage system. The findings quantitatively demonstrate the influence of key design and operating parameters on system performance and provide optimization criteria relevant to engineering-scale applications.

1. Number of Reactors: Increasing the number of reactors was found to be one of the most significant factors enhancing system performance. The exergy efficiency (η_{ex}) increased from 21.5% for two reactors to 64.9% for six reactors. This improvement indicates that multi-reactor configurations are advantageous for industrial-scale hydrogen storage systems, as they enhance heat management and overall energy efficiency.
2. Outlet Temperature: As the outlet temperature increased, the absorption efficiency decreased. The η_{ex} value declined from 65.99% at 50 °C to 24.64% at 70 °C. This highlights the strong sensitivity of the absorption process to thermal balance and defines an optimal operating temperature range of 50–60 °C, which serves as a key reference for thermal management in MH reactor design.
3. Coolant Mass Flow Rate: Although increasing the coolant flow rate improves heat transfer, it simultaneously raises pump power losses, reducing overall efficiency. At 0.5 kg/s, η_{ex} was 49.13%, but it fell to 16.38% at 1.5 kg/s. These results suggest that operating at low-to-moderate flow rates provides a better energy–exergy trade-off and that pump design should consider both thermodynamic and economic performance.
4. Pump Efficiency: Increasing pump efficiency from 60% to 80% slightly raised η_{ex} from 24.78% to 24.96%. Although the gain is modest, improving auxiliary equipment efficiency has a positive cumulative effect on overall system performance. Therefore, the use of high-efficiency pumps and circulation units is recommended to minimize long-term operational losses.
5. Ambient Temperature: When the ambient temperature rose from 20 °C to 30 °C, η_{ex} decreased marginally from 24.94% to 24.79%. While this variation is relatively small, it shows that environmental conditions have a measurable effect on thermodynamic behavior. Thus, MH storage systems should be thermally insulated and climate-adapted to mitigate environmental fluctuations.
6. Heat Transfer Coefficient The heat transfer coefficient (h) exhibited the strongest influence on system performance. When h increased from 1000 W/m²·K to 3000 W/m²·K, η_{ex} improved markedly from 24.64% to 73.91%. This confirms that effective heat removal is the dominant factor controlling hydrogen absorption. Therefore, advanced heat exchanger designs—such as multi-tube reactors, conical exchangers, or PCM-integrated systems—should be prioritized in MH reactor engineering.
7. Hydrogen Storage Capacity: Enhancing hydrogen loading capacity (C_H_2) significantly increased system efficiency. When C_H_2 rose from 20 mol/kg to 40 mol/kg, η_{ex} increased from 6.55% to 13.09%. This finding underscores the importance of high-capacity MgH_2-based and hybrid materials. In materials engineering, capacity improvements achieved through nanostructuring or alloying directly enhance both performance and design flexibility.
8. Volume-to-Surface Area Ratio (V/A): As the V/A ratio increased, heat transfer deteriorated, leading to lower exergy efficiency. At V/A = 0.05 m, η_{ex} was 2.33%, while at V/A = 0.10 m, it dropped to 1.17%. Lower V/A ratios promote better internal heat distribution and faster absorption. Therefore, maintaining a low V/A ratio is essential for improving heat transfer and reactor performance.

Engineering Applications and Future Work:

The results identify the most critical parameters governing the design and scalability of MH-based hydrogen storage systems. Among these, the number of reactors, heat transfer coefficient, and hydrogen storage capacity are dominant factors determining energy and exergy performance.
Future research should integrate economic and environmental assessments into the present model, explore hybrid heat management concepts (e.g., PCM-assisted, nanofluid, or multi-channel designs), and develop automated control and optimization algorithms for dynamic operation.
By incorporating these developments, MgH_2-based systems can evolve into next-generation, high-efficiency, and sustainable hydrogen storage technologies suitable for large-scale clean energy applications. Within this context, parameters such as reactor number, pump efficiency, and the V/A ratio were jointly evaluated under a multi-parametric exergy framework. This integrated approach contributes to the limited literature addressing these interactions simultaneously, and the results are expected to serve as a reference for future optimization and design studies on metal hydride-based hydrogen storage systems.

Ethics Committee Approval and Conflict of Interest Statement

There is no need to obtain permission from the ethics committee for the article prepared.
There is no conflict of interest with any person / institution in the article prepared.

Authors' Contributions

Beyazit İlgin: Study conception and design; Acquisition of data; Analysis and interpretation of data; Drafting of manuscript; Critical revision.

Acknowledgement

Not applicable.

References

[1] İ. Dinçer and C. Acar, "Review and evaluation of hydrogen production methods for better sustainability," International Journal of Hydrogen Energy, vol. 40, no. 34, p. 11094, Jan. 2015, doi: 10.1016/j.ijhydene.2014.12.035.

[2] M. Ball and M. Weeda, "The hydrogen economy – Vision or reality?," International Journal of Hydrogen Energy, vol. 40, no. 25, p. 7903, May 2015, doi: 10.1016/j.ijhydene.2015.04.032.

[3] M. Lototskyy, V. A. Yartys, B. G. Pollet, and R. C. Bowman, "Metal hydride hydrogen compressors: A review," International Journal of Hydrogen Energy, vol. 39, no. 11, p. 5818, Feb. 2014, doi: 10.1016/j.ijhydene.2014.01.158.

[4] L. Schlapbach and A. Züttel, "Hydrogen-storage materials for mobile applications," Nature, vol. 414, no. 6861, p. 353, Nov. 2001, doi: 10.1038/35104634.

[5] A. Züttel, "Hydrogen storage methods," The Science of Nature, vol. 91, no. 4, p. 157, Apr. 2004, doi: 10.1007/s00114-004-0516-x.

[6] B. Sakintuna, F. Lamari-Darkrim, and M. Hirscher, "Metal hydride materials for solid hydrogen storage: A review," International Journal of Hydrogen Energy, vol. 32, no. 9, p. 1121, Jan. 2007, doi: 10.1016/j.ijhydene.2006.11.022.

[7] I. P. Jain, C. Lal, and A. Jain, "Hydrogen storage in Mg: A most promising material," International Journal of Hydrogen Energy, vol. 35, no. 10, p. 5133, Oct. 2009, doi: 10.1016/j.ijhydene.2009.08.088.

[8] R. Paramonov, T. Spassov, P. Nagy, and Á. Révész, "Synergetic Effect of FeTi in Enhancing the Hydrogen-Storage Kinetics of Nanocrystalline MgH2," Energies, vol. 17, no. 4, p. 794, Feb. 2024, doi: 10.3390/en17040794.

[9] A. K. Patel et al., "Study of the Microstructural and First Hydrogenation Properties of TiFe Alloy with Zr, Mn and V as Additives," Processes, vol. 9, no. 7, p. 1217, Jul. 2021, doi: 10.3390/pr9071217.

[10] L. Ren et al., "Nanostructuring of Mg-Based Hydrogen Storage Materials: Recent Advances for Promoting Key Applications," Nano-Micro Letters, vol. 15, no. 1, Apr. 2023, doi: 10.1007/s40820-023-01041-5.

[11] A. Mohammadi et al., "High-entropy hydrides for fast and reversible hydrogen storage at room temperature," Acta Materialia, vol. 236, p. 118117, Jun. 2022, doi: 10.1016/j.actamat.2022.118117.

[12] S. Dangwal and K. Edalati, "High-entropy alloy TiV2ZrCrMnFeNi for hydrogen storage at room temperature," Scripta Materialia, vol. 238, p. 115774, Sep. 2023, doi: 10.1016/j.scriptamat.2023.115774.

[13] Y. Kozhakhmetov et al., "High-Entropy Alloys: Innovative Materials with Unique Properties for Hydrogen Storage," Metals, vol. 15, no. 2, p. 100, Jan. 2025, doi: 10.3390/met15020100.

[14] V. K. Kukkapalli, S. Kim, and S. A. Thomas, "Thermal Management Techniques in Metal Hydrides for Hydrogen Storage Applications: A Review," Energies, vol. 16, no. 8, p. 3444, Apr. 2023, doi: 10.3390/en16083444.

[15] G. Miao et al., "Review of thermal management technology for metal hydride reaction beds," Sustainable Energy & Fuels, vol. 7, no. 9, p. 2025, 2023, doi: 10.1039/d2se01690g.

[16] P. Larpruenrudee et al., "The enhancement of metal hydride hydrogen storage performance using novel triple-branched fin," Journal of Energy Storage, vol. 123, p. 116659, Apr. 2025, doi: 10.1016/j.est.2025.116659.

[17] R. Ran, J. Wang, F. Yang, and R. Imin, "Fast Design and Numerical Simulation of a Metal Hydride Reactor," Energies, vol. 17, no. 3, p. 712, Feb. 2024, doi: 10.3390/en17030712.

[18] V. N. Kudiiarov, R. R. Elman, N. S. Pushilina, and N. Kurdyumov, "State of the Art in Development of Heat Exchanger Geometry Optimization," Materials, vol. 16, no. 13, p. 4891, Jul. 2023, doi: 10.3390/ma16134891.

[19] S. Jana and P. Muthukumar, "Design, development and hydrogen storage performance testing of a tube bundle metal hydride reactor," Journal of Energy Storage, vol. 63, p. 106936, Mar. 2023, doi: 10.1016/j.est.2023.106936.

[20] G. Mohan, M. P. Maiya, and S. Srinivasamurthy, "Performance simulation of metal hydride hydrogen storage device," International Journal of Hydrogen Energy, vol. 32, no. 18, p. 4978, Oct. 2007, doi: 10.1016/j.ijhydene.2007.08.007.

[21] S. Parashar, P. Muthukumar, and A. K. Soti, "Experimental study on absorption and desorption behavior of a novel metal hydride reactor," International Journal of Hydrogen Energy, vol. 94, p. 1224, Nov. 2024, doi: 10.1016/j.ijhydene.2024.11.058.

[22] M. Raju and S. Kumar, "Optimization of heat exchanger designs in metal hydride based hydrogen storage systems," International Journal of Hydrogen Energy, vol. 37, no. 3, p. 2767, Aug. 2011, doi: 10.1016/j.ijhydene.2011.06.120.

[23] X.-S. Bai et al., "Optimization of tree-shaped fin structures towards enhanced absorption performance," Energy, vol. 220, p. 119738, Dec. 2020, doi: 10.1016/j.energy.2020.119738.

[24] Y. Liu et al., "Numerical investigation of metal hydride heat storage reactor with multiple tubes," Energy, vol. 253, p. 124142, May 2022, doi: 10.1016/j.energy.2022.124142.

[25] V. Pandey, K. V. Krishna, and M. P. Maiya, "Numerical modelling and heat transfer optimization of large-scale reactors," International Journal of Hydrogen Energy, vol. 48, no. 42, p. 16020, Jan. 2023, doi: 10.1016/j.ijhydene.2023.01.058.

[26] S. Shafiee, "Operational principles and effect of operating parameters on performance of metal hydride heat pumps," International Journal of Refrigeration, vol. 120, p. 22, Aug. 2020, doi: 10.1016/j.ijrefrig.2020.08.025.

[27] S. N. Nyamsi and I. Tolj, "The Impact of Active and Passive Thermal Management," Energies, vol. 14, no. 11, p. 3006, May 2021, doi: 10.3390/en14113006.

[28] I. Dincer and M. A. Rosen, Exergy: energy, environment and sustainable development. Newnes, 2012. Available: http://ci.nii.ac.jp/ncid/BA8326393X

[29] Y. A. Cengel and M. A. Boles, Thermodynamics: An engineering approach, 8th ed. McGraw-Hill Education, 2015.

[30] V. Bahrs, F. Franke, S. Kazula, and S. de Graaf, "Analysis of the potential of metal hydride-based range extenders," CEAS Aeronautical Journal, Dec. 2024, doi: 10.1007/s13272-024-00784-0.

[31] T. L. Bergman, Fundamentals of heat and mass transfer. John Wiley & Sons, 2011. [Online]. Available: https://ci.nii.ac.jp/ncid/BB01294600

[32] B. Galey et al., "Improved hydrogen storage properties of Mg/MgH2," International Journal of Hydrogen Energy, vol. 44, no. 54, p. 28848, Oct. 2019, doi: 10.1016/j.ijhydene.2019.09.127.

-[33] Y. A. Cengel and J. M. Cimbala, Fluid mechanics: Fundamentals and applications, 3rd ed. McGraw-Hill Education, 2014.

[34] A. Bejan, Advanced engineering thermodynamics, 4th ed. John Wiley & Sons, 2016, doi: 10.1002/9781119245964.

[35] S. Parashar, P. Muthukumar, and A. K. Soti, "Design optimization and numerical investigation," Thermal Science and Engineering Progress, vol. 49, p. 102468, Feb. 2024, doi: 10.1016/j.tsep.2024.102468.

[36] A. H. Eisapour et al., "Enhancing hydrogen storage efficiency," International Journal of Hydrogen Energy, vol. 109, p. 1090, Feb. 2025, doi: 10.1016/j.ijhydene.2025.02.146.

-[37] F. Askri et al., "Numerical investigation of high temperature metal hydride water pumping system," International Journal of Hydrogen Energy, vol. 44, no. 31, p. 16777, May 2019, doi: 10.1016/j.ijhydene.2019.04.263.

[38] T. Alqahtani, S. Mellouli, F. Askri, S. Algarni, B. M. Alshammari, and L. Kolsi, "Numerical Investigation on Thermal Performance of Three Configurations of Solar Thermal Collector Integrated with Metal Hydride," Case Studies in Thermal Engineering, p. 105314, Oct. 2024, doi: 10.1016/j.csite.2024.105314.

[39] I. Ayub et al., "Performance improvement of solar bakery unit," Renewable Energy, vol. 161, p. 1011, Aug. 2020, doi: 10.1016/j.renene.2020.07.133.

[40] P. Krane et al., "Dynamic modeling and control of a two-reactor metal hydride energy storage system," Applied Energy, vol. 325, p. 119836, Sep. 2022, doi: 10.1016/j.apenergy.2022.119836.

[41] P. Krane et al., "Assessment of metal-hydride energy storage coupled with heat pumps and solar PV," Purdue Univ., 2021. [Online]. Available: https://docs.lib.purdue.edu/cgi/viewcontent.cgi?article=1372&context=ihpbc.

[42] T. Alqahtani et al., "Numerical Investigation on Thermal Performance of Solar Collector with Metal Hydride," Case Studies in Thermal Engineering, p. 105314, Oct. 2024, doi: 10.1016/j.csite.2024.105314.